Bull. Mater. Sci., Vol. 34, No. 7, December 2011, pp. 1617–1625. © Indian Academy of Sciences.

Structural, elastic and thermodynamic properties of Ti_2SC

HONGZHI FU[1,2,*], WENFANG LIU[3] and TAO GAO[4]

[1]College of Physics and Electronic Information, Luoyang Normal College, Luoyang 471022, P.R. China
[2]National Laboratory of Superhard Materials, Jilin University, Changchun 130012, P.R. China
[3]College of Chemistry and Chemical Engineering, Luoyang Normal College, Luoyang 471022, P.R. China
[4]Institute of Atomic and Molecular Physics, Sichuan University, Chengdu 610065, P.R. China

MS received 17 June 2010

Abstract. **The structural parameters, elastic constants and thermodynamic properties of Ti_2SC were investigated under pressure and temperature by using first-principles plane-wave pseudopotential density functional theory within the generalized gradient approximation. The obtained results are in agreement with the available experimental data. The bulk moduli along the *a*- and *c*-axes, B_a and B_c, almost linearly increase with pressure, and the former is always smaller than the latter. The ratio of B_c/B_a has a trend of gradual increase as the pressure increases. It is found that the elastic constants, anisotropy and Debye temperature of Ti_2SC increase with pressure, while axial compressibility along the *a*- and *c*-axes decreases with pressure. The thermal properties including the equation of state, the Grüneisen parameter γ, the anisotropies Δ_p, Δ_{S1} and Δ_{S2}, and the heat capacity are estimated at various pressures and temperatures.**

Keywords. **Ti_2SC; elastic properties; thermodynamic properties; *Ab initio* calculations.**

1. Introduction

Ti_2SC is a member of a class of materials which are now widely referred to as the $M_{n+1}AX_n$ phases, where n is 1, 2, or 3 and M represents an early transition metal, A is an A-group element (mostly IIIA and IVA element), and X is either carbon and/or nitrogen (Barsoum 2000). Like metals, which are not susceptible to thermal shock, they are electrically and thermally conductive, plastic at high temperature, exceptionally damage tolerant and most readily machinable. Like ceramics, they are elastically rigid, lightweight, fatigue resistant and maintain their strengths to high temperatures (Drulis *et al* 2007). These make them attractive for many applications such as structural materials at elevated temperature. $M_{n+1}AX_n$ compounds crystallize under a hexagonal structure with a very large *c/a* ratio. Based on the value of n, this class of materials can be further classified as M_2AX or 211 MAX compounds ($n = 1$), M_3AX_2 or 321 MAX compounds and M_4AX_3 or 413 MAX compounds ($n = 3$). More than 50 compounds were reported for $n = 1$, the so-called M_2AX phases. Interestingly, Ti_2SC has the ease of machinability among the titanium alloys (Wally and Ueki 1998; Tetsuya *et al* 2002). With Vicker's hardness of 8 GPa (Barsoum and Raghy 1996, 1997, 1999), it is relatively soft as compared to most other early transition metal carbides and nitrides. Like the rest of the M_2AX phases, Ti_2SC belongs to a Raman-active material and has a total of 24 modes out of which three are acoustic (A2u + Eu), four are Raman-active optical, three of which are Raman-active (Ag + 2E2g) (Spanier *et al* 2005). The M_2AX phases belong to the space group *P63/mmc* and have nearly close-packed M layers which are sandwiched by layers of the A-group element, with the X atoms occupying the octahedral sites and forming edge-shared XM_6 octahedra (Yang *et al* 2006). It is interesting that Ti_2SC has a significantly shorter *c*-lattice parameter among the 50 other MAX phases, and was postulated that its mechanical properties would be significantly different than the others. At 8 ± 2 GPa, its steady state Vicker's hardness is significantly higher than the vast majority of MAX phases whose hardness are in the range of 2–4 GPa. Furthermore, at 316 ± 2 GPa, its Young's modulus is the highest one among M_2AX phase (Amini *et al* 2007). Ti_2SC also exhibits the highest thermal conductivity at room temperature (> 60 W/mK) and the Poisson ratio (0·199), which were attributed, respectively, to higher phonon conduction and bond anisotropy as compared to other 211 MAX phases (Scabarozi *et al* 2008). However, Ti_2SC did not show any significant difference in the high-pressure behaviour (Kulkarni *et al* 2008) as compared to the other MAX phases (Manoun *et al* 2006).

Unfortunately, Ti_2SC has been less investigated compared to the other members of this family. Experimen-

*Author for correspondence (fhzscdx@163.com)

tally, Kulkarni and co-workers (2008) investigated the pressure dependence of the lattice parameters of Ti_2SC by using synchrotron radiation X-ray diffraction and a diamond anvil cell setup. Amini *et al* (2007) and Kulkarni *et al* (2009) reported the synthesis and mechanical properties of Ti_2SC. Theoretically, Hug (2006), Du *et al* (2008) and Bouhemadou and Khenata (2008) studied the electronic structure of Ti_2SC using *ab initio* calculations. Recently, the hardness and brittleness and thermal expansion are investegated by Cui *et al* (2009) and Scabarozi *et al* (2009) respectively. From above, it is clear that some fundamental properties of Ti_2SC have not been investigated, and the elastic and thermal properties are rarely studied or measured for Ti_2SC.

Elastic properties are important not only because they are closely related to various fundamental solid-state phenomena such as interatomic bonding, equations of state and phonon spectra, but also because they link thermodynamically with the specific heat, thermal expansion, Debye temperature, melting point and Grüneisen parameter. Values of elastic constants can not only provide valuable information about the bonding characteristic between adjacent atomic planes but also the anisotropic character of the bonding and structural stability, as well as the correlation between the elastic constants and the melting temperature. It is known that pressure is an important parameter to tune physical properties, because they have already displayed many marvelous physics phenomenon recently (Ma *et al* 2009). In this work, we investigate elastic properties and thermal properties of Ti_2SC under pressure and temperature using the first-principles plane-wave method. The motivations of this study are to determine the elastic and thermal behaviour of Ti_2SC, and to investigate if it exhibits any unusual behaviour under high pressure.

2. Computational details

The thermal properties and elastic properties calculations were performed using the pseudopotential plane-wave method within the framework of the density functional theory (Milman *et al* 2000; Segall *et al* 2002). This technique has become widely recognized as the method for studying physical properties of the condensed materials (Lippens *et al* 2008). The thermodynamic properties for Ti_2SC are calculated by the quasi-harmonic Debye model (Blanco *et al* 2004). The exchange correlation energy is described in the generalized gradient approximation (GGA) using the Perdew–Burke–Ernzerhof (PBE) functional (Perdew *et al* 1996). The Ti ($3d^24s^2$), S ($3s^23p^6$) and C ($2s^22p^2$) states are treated as valence electrons. Interactions of electrons with ion cores are presented by the norm-conserving pseudopotential for all atoms. In all the high-precision calculations, the cut-off energy of the plane-wave basis set is to 350 eV for Ti_2SC. The special points sampling integration over the Brillouin zone are carried out using the Monkhorst–Pack method with a $9 \times 9 \times 2$ special k-point mesh. The kinetic energy cut-off and mesh of k-points are optimized by performing self-consistent calculations. The self-consistent is considered to be converged when the total energy is 10^{-6} eV/atom. These parameters are sufficient in leading to well-converged total energy calculations.

3. Results and discussion

3.1 *Structural properties*

The total energy electronic structure calculations are performed over a range of primitive cell volume V from $0{\cdot}6\ V_0$ to $1{\cdot}20\ V_0$, where V_0 is the zero pressure equilibrium primitive cell volume. No constraints are imposed on the c/a ratio, i.e. the lattice constants a and c are optimized simultaneously. Since the experimental c/a ratio of Ti_2SC is about 3·494, we calculate a series of different c/a ratios from 3·474 to 3·514, with a step of 0·004. For each volume, we determine the corresponding equilibrium ratio c/a of Ti_2SC by performing total energy calculations on a series of different c/a ratios and minimize the energy as function of c/a. Through these calculations, we can obtain the equilibrium parameters a and c and the corresponding equilibrium ratio c/a of Ti_2SC under arbitrary pressures. We plot ratio V/V_0 varies with pressure in figure 1 together with experimental results (Kulkarni *et al* 2008, 2009), which shows better consistency in unit cell volume. However, our calculated relative change in unit cell is smaller than that in Kulkarni *et al* (2009). We attribute these to the different pseudo potential, because the generalized gradient approximation (GGA) always overestimates the lattice constant and local density approximation (LDA) underestimates the lattice constant. It is noted that the most stable structure of the Ti_2SC corresponds to the ratio $c/a = 3{\cdot}5139$, where $a = 3{\cdot}2044$ Å and $c = 11{\cdot}2601$ Å, listed in table 1, together with other theoretical (Bouhemadou and Khenata 2008; Du *et al* 2008) and experimental (Amini 2007; Kulkarni 2008, 2009) data. The zero pressure bulk modulus B_0 and the derivative B_0' of the bulk modulus with respect to pressure obtained from the Birch–Murnaghan equation of state (EOS) (Murnaghan 1994), are also shown in table 1. In order to study further, the pressure/temperature dependence of unit cell parameters, volume and their ratios, respectively, of Ti_2SC are also calculated and given in tables 2 and 3, copmparing with the experimental (Kulkarni *et al* 2008, 2009) data. It is clear that our results are in good agreement with the experimental data.

We notice that, when pressure increases, the compression along the c-axis is smaller than that along the a-axis (not shown), reflecting change of Ti–S, Ti–C and C–C bond with the applied pressures. This result is important, since to a first approximation the vibrational frequencies

Table 1. Calculated structure parameters, bulk modulus B (GPa) and its pressure derivation B' (GPa), shear modulus G (GPa), Young's modulus E (GPa), Poisson's ratio σ, thermal expansion α (10^{-5} K^{-1}), Grüneisen parameter γ and elastic constants C_{ij} (GPa) of Ti_2SC compared with the experimental and theoretical results.

	a (Å)	c (Å)	c/a	B	B'	C_{11}	C_{12}	C_{13}	C_{33}	C_{44}	G	σ	E	α	γ
This work	3·204	11·26	3·514	178	4·07	332	93	101	355	156	134	0·199	321	1·082	1·88
Du *et al* (2008)	3·211	11·239	3·500	181		336	106	99	348	163					
Bouhemadou and Khenata (2008)	3·1432	11·0509	3·5159	205	4·22	368	108	123	395	189	150·8	0·203	363		
Cui *et al* (2009)	3·206	11·236	3·505	179	4·13	318	101	105	351	148	124	0·219	302		
Scabarozi *et al* 2009	3·2046	11·209	3·498	179		339	90	100	354	162	139	0·192	331	0·87	1·40
Kulkarni *et al* 2008	3·208	11·21	3·4944	191	4·0	–	–								
Amini *et al* 2007	3·205	11·208	4·497	–	–	–	–								
Kulkarni *et al* 2009	3·208	11·21	3·4944												

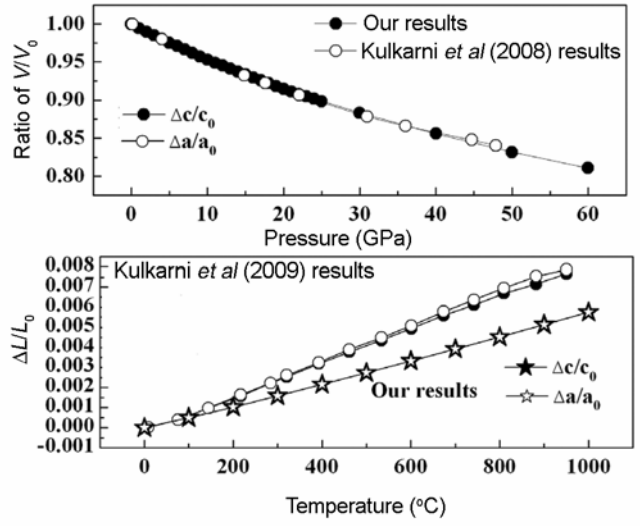

Figure 1. The normalized ratio (V/V_0 and $\Delta L/L_0$) as a function of pressure and temperature.

are dependent on bond distances. As expected experimentally and theoretically, the Ti–S, Ti–C and C–C bond lengths decrease with pressure. Moreover, the atoms in the interlayers become closer, and the interactions between them become stronger; contraction of Ti–S, Ti–C and C–C distances under pressure results in the change of bonding anisotropy of Ti_2SC structure. The interlayer linear compressibility $d\ln a/d\ln p = 0{\cdot}00194$ GPa^{-1} is about 1·13 times larger than $d\ln c/dp = 0{\cdot}00171$ GPa^{-1}, showing the Ti–S bond and C–C bond to be different.

3.2 *Elastic properties*

To calculate the elastic constants under pressure, we have applied the non-volume-conserving method. The complete elastic constant tensor was determined from calculations of the stresses induced by small deformations of the equilibrium primitive cell, and thus the elastic constants c_{ijkl} are determined as (Karki *et al* 1997)

$$c_{ijkl} = \left(\frac{\partial \sigma_{ij}(x)}{\partial e_{kl}}\right)_X, \tag{1}$$

where σ_{ij} and e_{kl} are applied stress and Eulerian strain tensors, X and x are the coordinates before and after the deformation. For the isotropic stress, the elastic constants are defined as (Wallace 1972)

$$c_{ijkl} = C_{ijkl} + \frac{P}{2}(2\delta_{ij}\delta_{kl} - \delta_{il}\delta_{jk} - \delta_{ik}\delta_{jl}), \tag{2}$$

$$C_{ijkl} = \left(\frac{1}{V(x)}\frac{\partial^2 E(x)}{\partial e_{ij}\partial e_{kl}}\right)_X, \tag{3}$$

where C_{ijkl} are the second-order derivatives with respect to the infinitesimal strain. For Ti_2SC, there are five independent elastic constants. It is shown that our results (table 1) are consistent with other theoretical data (Bouhemadou and Khenata 2008; Du *et al* 2008). The obtained values of C_{11}, C_{12}, C_{13}, C_{33} and C_{44} at zero temperature (up to 50 GPa) are shown in figure 2. We found that the five independent elastic constants increase monotonically with pressure. C_{11} and C_{33} vary rapidly as pressure increases, and C_{44} becomes moderate as well as C_{13}. However, C_{12} increases comparatively slowly. Unfortunately, there are no experimental and theoretical data to compare our results. The five independent elastic constants satisfy the well-known Born stability criteria (Born 1940), i.e.

$$C_{12} > 0, \quad C_{33} > 0, \quad C_{66} = (C_{11} - C_{12})/2 > 0, \quad C_{44} > 0, \tag{4}$$

and

$$(C_{11} + C_{12})C_{33} - 2C_{13}^2 > 0. \tag{5}$$

This suggests that the Ti_2SC is mechanically stable and predicts that there is not a phase transition up to 50 GPa.

The mechanical anisotropy of Ti_2SC can be calculated using the bulk moduli along the a and c axes, B_a and B_c respectively, defined as (Islam *et al* 2006)

Table 2. The pressure dependence of unit cell parameters, volume and their ratios, respectively of Ti_2SC.

	Kulkarni *et al* 2008						Calculated					
P(GP)	*a* (Å)	*c* (Å)	*V* (Å^3)	a/a_0	c/c_0	V/V_0	*a* (Å)	*c* (Å)	*V* (Å^3)	a/a_0	c/c_0	V/V_0
0	3·208	11·21	99·9	1	1	1	3·21303	11·27704	100·82	1	1	1
4·067	3·191	11·11	98	0·9947	0·99108	0·98098	3·18779	11·19892	98·56	0·99214	0·99307	0·97753
13·92	3·151	10·92	93·9	0·98223	0·97413	0·93994	3·13476	11·04491	93·99	0·97564	0·97942	0·93224
17·33	3·132	10·84	92	0·97631	0·96699	0·92092	3·11863	11·00052	92·66	0·97062	0·97548	0·919
21·86	3·116	10·77	90·5	0·97132	0·96075	0·90591	3·09823	10·94487	90·98	0·96427	0·97054	0·90243
23·57	3·115	10·76	90·4	0·97101	0·95986	0·9049	3·09117	10·92403	90·4	0·96207	0·9687	0·89661
30·87	3·087	10·63	87·7	0·96228	0·94826	0·87788	3·06213	10·84676	88·08	0·95303	0·96184	0·87362
35·74	3·074	10·58	86·6	0·95823	0·9438	0·86687	3·04428	10·79893	86·67	0·94748	0·9576	0·85966
44·24	3·044	10·54	84·684	0·94888	0·94023	0·84769	3·01549	10·72458	84·455	0·93852	0·95101	0·83766
45·68	3·046	10·55	84·8	0·9495	0·94112	0·84885	3·01098	10·71108	84·1	0·93712	0·94981	0·83411
47·58	3·037	10·49	83·8	0·9467	0·93577	0·83884	3·00484	10·69684	83·64	0·93521	0·94855	0·82961

Table 3. The temperature dependence of unit cell parameters, volume and their ratios, respectively, of Ti_2SC.

Kulkarni *et al* (2009) *T* (°C)	*a* (Å) (± 0·001)	*c* (Å) (± 0·003)	*V* (Å^3) (± 0·1)	$\Delta a/a_0$	$\Delta c/c_0$	$\Delta V/V_0$
25	3·209	11·210	99·9	0	0	0
92(2)	3·210	11·214	100·0	0·0004	0·0004	0·0011
160(2)	3·212	11·220	100·2	0·0010	0·00098	0·0029
229(3)	3·214	11·228	100·4	0·0016	0·00162	0·0047
298(3)	3·216	11·235	100·6	0·0022	0·00224	0·0066
332(4)	3·217	11·239	100·7	0·0025	0·00261	0·0076
401(4)	3·219	11·246	100·9	0·0032	0·0032	0·0096
469(5)	3·221	11·253	101·0	0·0038	0·00391	0·0114
538(5)	3·222	11·260	101·2	0·0044	0·00451	0·0132
606(6)	3·224	11·266	101·4	0·0049	0·00509	0·0150
675(6)	3·226	11·274	101·6	0·0056	0·00576	0·0170
744(7)	3·228	11·280	101·8	0·0061	0·00635	0·0185
812(8)	3·230	11·287	101·9	0·0067	0·00696	0·0204
881(8)	3·231	11·294	102·1	0·0071	0·00759	0·0219
949(9)	3·233	11·297	102·2	0·0076	0·00780	0·0232
Our work *T* (°C)	*a* (Å)	*c* (Å)	*V* (Å^3)	$\Delta a/a_0$	$\Delta c/c_0$	$\Delta V/V_0$
0	3·20837	11·2607	100·50171	0	0	0
100	3·20996	11·26628	100·65138	0·00049	0·00049	0·00149
200	3·21168	11·27231	100·8129	0·00103	0·00103	0·0031
300	3·21347	11·2786	100·98183	0·00159	0·00159	0·00478
400	3·21529	11·28499	101·15373	0·00216	0·00216	0·00649
500	3·21716	11·29155	101·33007	0·00274	0·00274	0·00824
600	3·21903	11·2981	101·50641	0·00332	0·00332	0·01
700	3·22094	11·3048	101·68719	0·00392	0·00392	0·0118
800	3·22288	11·3116	101·87094	0·00452	0·00452	0·01362
900	3·22483	11·31846	102·05617	0·00513	0·00513	0·01547
1000	3·22681	11·32541	102·24436	0·00575	0·00575	0·01734

$$B_a = a\frac{dP}{da} = \frac{\Lambda}{2+\alpha}, \tag{6}$$

$$B_c = c\frac{dP}{dc} = \frac{B_a}{\alpha}, \tag{7}$$

$$\Lambda = 2(C_{11}+C_{12}) + 4C_{13}\alpha + C_{33}\alpha^2, \tag{8}$$

$$\alpha = \frac{C_{11}+C_{12}-2C_{13}}{C_{33}-C_{13}}. \tag{9}$$

The calculated B_a and B_c with pressure are presented in figure 3. It can be seen that B_a and B_c almost linearly increase with pressure, and the former is always smaller than the latter. It is interesting that the ratio of B_c/B_a has a trend of gradual increase as the pressure increases, showing that the mechanical behaviour of Ti_2SC is of anisotropy under pressure.

It is known that the acoustic velocities are obtained from elastic constants by the Christoffel equation (Auld 1973)

$$(C_{ijkl}\, n_j n_k - M\delta_{il})\mu_i = 0, \tag{10}$$

where $M = \rho v^2$, C_{ijkl} is the fourth-rank tensor description of the elastic constants, n is the propagation direction and μ is the polarization vector; the acoustic anisotropy is defined as (Neumann *et al* 1999)

$$\Delta_i = \frac{M_i[n_x]}{M_i[100]}, \tag{11}$$

where n_x is the extremal propagation direction and i is the index of three types of elastic waves (one longitudinal and two traversal polarizations of shear waves). By solving the Christoffel (11) for hexagonal Ti_2SC, the anisotropy of the compression wave is obtained from (Steinle-Neumann *et al* 1999)

$$\Delta_P = \frac{V_l^2(0°)}{V_l^2(90°)} = \frac{C_{33}}{C_{11}}, \tag{12}$$

The anisotropies of the wave polarized perpendicular to the basal plane ($S1$) and to the basal plane ($S2$) are calculated (Steinle-Neumann *et al* 1999)

$$\Delta_{S1} = \frac{C_{11} + C_{33} - 2C_{13}}{4C_{44}}, \quad \Delta_{s2} = \frac{V_t^2(0°)}{V_t^2(90°)} = \frac{2C_{44}}{C_{11} - C_{12}}, \tag{13}$$

where Δ_P shows the anisotropy of the compression wave, Δ_{S1} and Δ_{S2} denote the shear waves, $V(90°)$ and $V(0°)$ are the in-plane and c-axis ultrasound velocities, respectively. For an elastically isotropic solid, $\Delta_P = \Delta_{s1} = \Delta_{s2} = 1$. The calculated pressure dependences of the anisotropies Δ_P, Δ_{S1} and Δ_{S2} are illustrated in figure 4. It is noted that Δ_{S2} increases rapidly and Δ_P increases slightly while increasing pressure. However, Δ_{S1} decreases with pressure (due to the fact that the elastic constants C_{11} and C_{33} are affected by pressure). The anisotropy is dependent on the symmetry of the crystal and the variations of the elastic constants, and the structure of the crystal has been changed because of the variations of c/a under applied pressures.

The expression for compressibility β for the hexagonal and rhombohedral systems can be written in matrix notation as (Sirdeshmukh *et al* 2001),

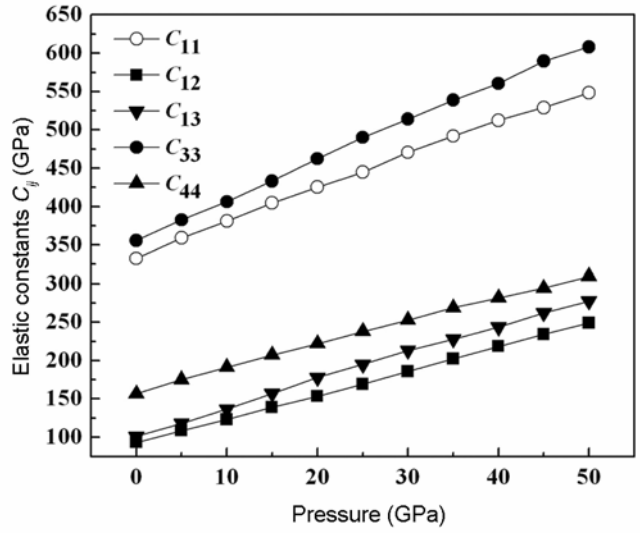

Figure 2. The elastic constants C_{ij} of Ti_2SC as a function of pressure.

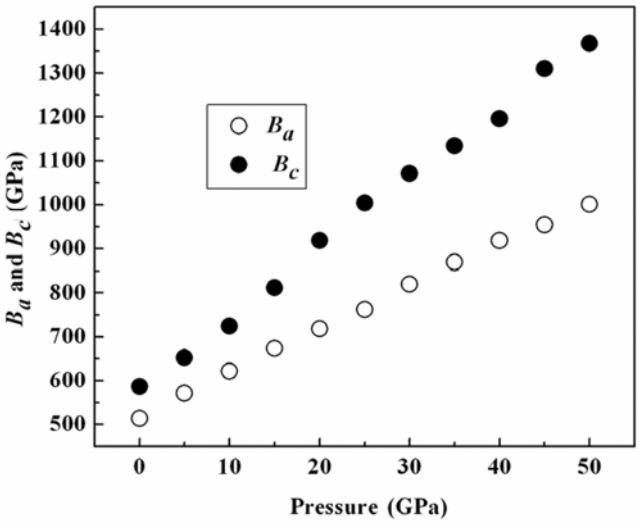

Figure 3. Variation of the bulk modulus B_a and B_c along the a- and c-axes with pressure.

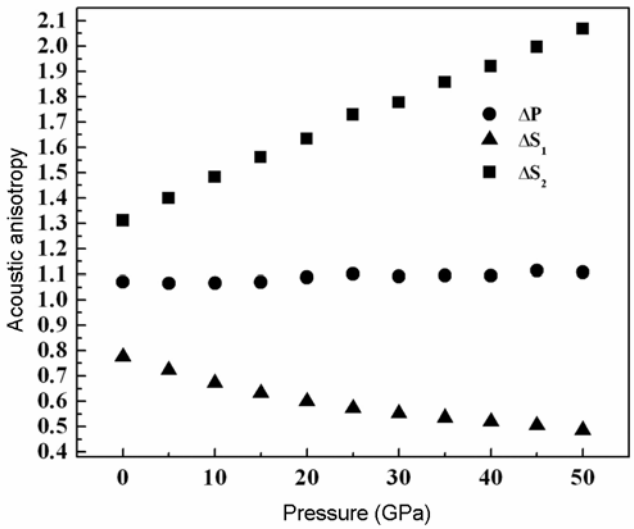

Figure 4. The anisotropies, elastic constant ratios C_{33}/C_{11}, $(C_{11} + C_{33} - 2C_{13})/4C_{44}$, $2C_{44}/(C_{11} - C_{12})$, which can determine the anisotropies of the compressional wave (ΔP) and the shear wave (ΔS_1 and ΔS_2), are displayed as functions of various pressures. The squares, circles and triangles represent ΔP, ΔS_1 and ΔS_2, respectively.

$$\beta = (S_{11} + S_{12} + S_{13}) - (S_{11} + S_{12} - S_{13} - S_{33})l^2. \quad (14)$$

where l is the unit directional vector ($l^2 = 0$ for c axis; $l^2 = 1$ for c axis) and S_{ij} is the elastic-compliance-constant. Thus, the linear compressibility in the uniaxial materials is rotationally symmetrical about the unique axis c. The pressure dependence of the lattice parameter is also related to a combination of elastic constants C_{ij}, and thus we can make use of the axial compressibility β to check the validity of the calculated S_{ij}. In a hexagonal crystal, the axial compressibilities β_a and β_c are of the form (Nye 1985)

$$\beta_a = -\mathrm{d}\ln a/\mathrm{d}P = \frac{C_{33} - C_{13}}{\Omega},$$

$$\beta_b = -\mathrm{d}\ln c/\mathrm{d}P = \frac{C_{11} + C_{12} - 2C_{13}}{\Omega}, \quad (15)$$

where $\Omega = (C_{11} + C_{12})C_{33} - 2C_{13}^2$.

Here, the β_a and β_c reflect the anisotropy of the linear compressibility. On the other hand, we can determine β_a and β_c by fitting a polynomial to the evolution of $\ln a$ and $\ln c$ at various pressures. The calculated β_a and β_c are 1·94 and 1·70 TGPa^{-1} (at 0 GPa), respectively, while the agreement with other calculated data (1·93 and 1·74 TGPa^{-1}) (Scabarozi *et al* 2009) are exact. The pressure effects on the axial compressibilities β_a and β_c are shown in figure 5. The axial β_a and β_c decrease with increasing pressure, but the β_a is always bigger than β_c. This also corresponds to the stronger bonding in Ti–S and weaker interlayer bonding in C–C.

3.3 *Thermodynamic properties*

With our previous works (Fu *et al* 2008a, b, 2009), we apply the quasi-harmonic Debye model to investigate the thermodynamic properties of Ti_2SC, in which the nonequilibrium Gibbs function $G^*(V; P, T)$ can be written in the form of (Francisco *et al* 1998; Blanco *et al* 2004)

$$G^*(V; P, T) = E(V) + PV + A_{\mathrm{Vib}}(\theta(V); T), \quad (16)$$

where $E(V)$ is the total energy per unit cell, PV corresponds to the constant hydrostatic pressure condition and $A_{\mathrm{Vib}}(\Theta(V); T)$ is the vibrational term, which can be written as

$$A_{\mathrm{Vib}}(\theta(V); T) = nKT\left[\frac{9\theta}{8T} + 3\ln(1 - e^{-\theta/T}) - D\left(\frac{\theta}{T}\right)\right], \quad (17)$$

where n is the number of atoms in the unit cell, K is the Boltzmann constant and the Debye integral $D(\Theta/T)$ is defined as (Blanco *et al* 2004)

$$D(y) = \frac{3}{y^3}\int_0^y \frac{x^3}{e^x - 1}\,\mathrm{d}x. \quad (18)$$

The heat capacity C_V and the thermal expansion (α) are expressed as

$$C_V = 3nK\left[4D(\theta/T) - \frac{3\theta/T}{e^{\theta/T} - 1}\right], \quad (19)$$

$$\alpha = \frac{\gamma C_V}{B_T V}, \quad (20)$$

where γ is the Grüneisen parameter defined as

$$\gamma = -\frac{\mathrm{d}\ln\theta(V)}{\mathrm{d}\ln V}. \quad (21)$$

The Debye temperature can be estimated from the average sound velocity v_m, using the following equation (Anderson 1963):

$$\theta = \frac{h}{k_B}\left(\frac{3nN_A\rho}{4\pi M}\right)^{1/3} v_m, \quad (22)$$

where h is Planck's constant, k_B is the Boltzmann constant, N_A is the Avogadro number, M is the molecule mass, ρ is the density and the average sound velocity v_m is approximately given by (Poirier 2000)

$$v_m = \left[\frac{1}{3}\left(\frac{2}{v_s^3} + \frac{1}{v_P^3}\right)\right]^{-1/3}, \quad (23)$$

where v_P and v_s are the longitudinal and transverse elastic wave velocities, respectively, which can be obtained from Navier's equation (Fu *et al* 2008b):

$$v_P = \sqrt{\left(B_S + \frac{4}{3}G\right)\Big/\rho}, \quad v_s = \sqrt{G/\rho}, \quad (24)$$

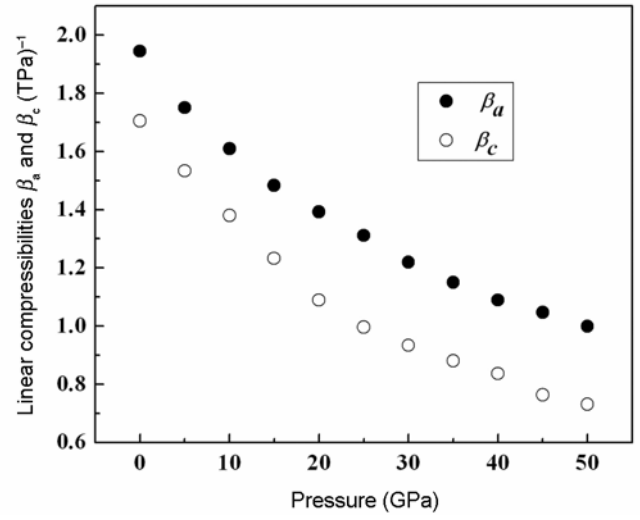

Figure 5. The linear compresibilities β_a and β_c plotted as a function of pressure.

where G is the shear modulus and B_S is the adiabatic bulk modulus.

In figure 6, we show the ratios of heat capacity C_V and the Debye temperature Θ as a function of pressure P at the temperatures of 300 and 800 K for Ti_2SC, where X_0 represents heat capacity and the Debye temperature at zero temperature. It is shown that when the temperature is constant, the Debye temperature Θ increases almost nonlinearly with applied pressures, indicating the change of the vibration frequency of particles under pressure. However, the heat capacity C_V decreases with the applied pressures, showing that the increasing pressure might achieve the same result with decreasing temperature in Ti_2SC. The variations of Θ with temperature T are plotted in figure 7. We can see that the Debye temperature Θ decreases by 1·9, 2·18 and 2·69% at the pressures of 0, 5 and 10 GPa, respectively, when the temperature is from 0 to 1000 K.

The Grüneisen parameter γ is thought to be described the alteration in a frequency of the crystal lattice vibration based on the lattice's increase or decrease in volume as the temperature changes. It is directly related to the equation of state (EOS). However, the agreement between our calculated value (1·88) and the other calculated data (1·40) (Scabarozi *et al* 2009) is not exact. They are shown in figure 8. It can be observed that at given pressure, the γ increases monotonously when $T > 500$ K (as shown in figure 8a); while at fixed temperature, the γ decreases dramatically with pressure, and as the temperature goes higher, the γ decreases more rapidly with the increase of pressure P (figure 8b). These results are due to the fact that the effect of temperature T on γ is not as significant as that of pressure P.

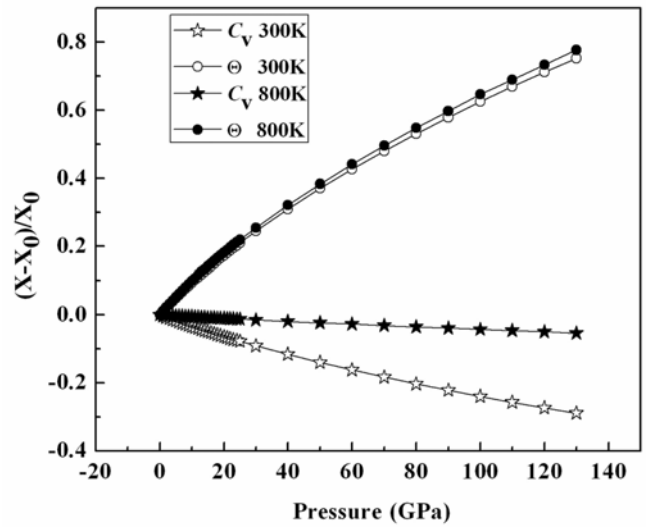

Figure 6. Variations of thermodynamic parameters X (X: Debye temperature or specific heat) with pressure P. They are normalized by $(X - X_0)/X_0$, where X and X_0 are the Debye temperature or heat capacity under any pressure P and zero pressure P_0 at the temperatures of 300 and 800 K.

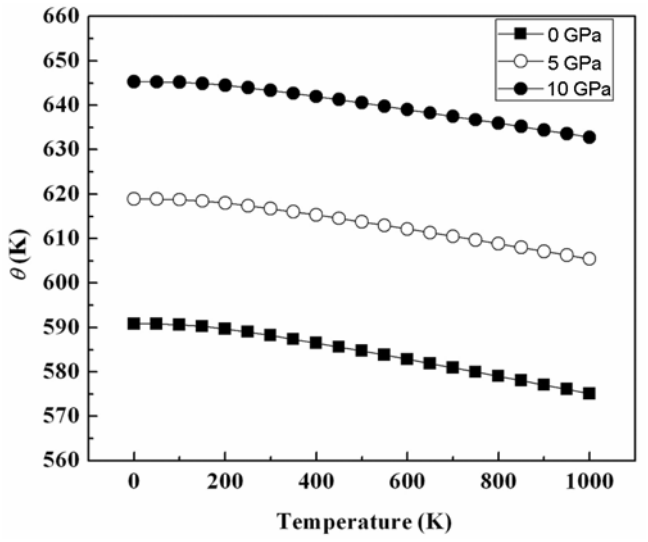

Figure 7. Variation of the Debye temperature Θ with the temperature at different pressures of P = 0, 5 and 10 GPa.

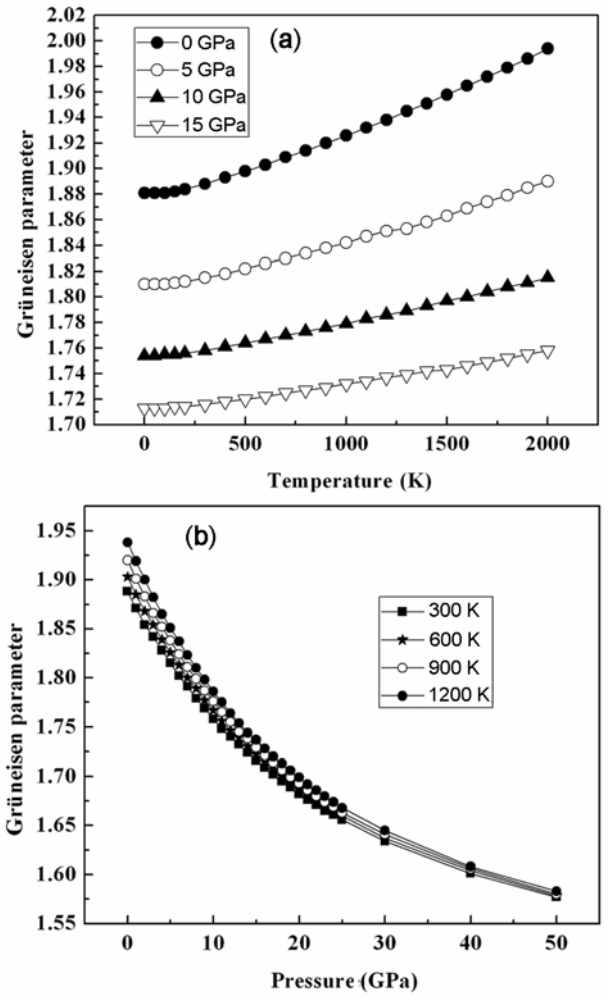

Figure 8. Variation of the Grüneisen parameter γ with (**a**) temperature T and (**b**) pressure P.

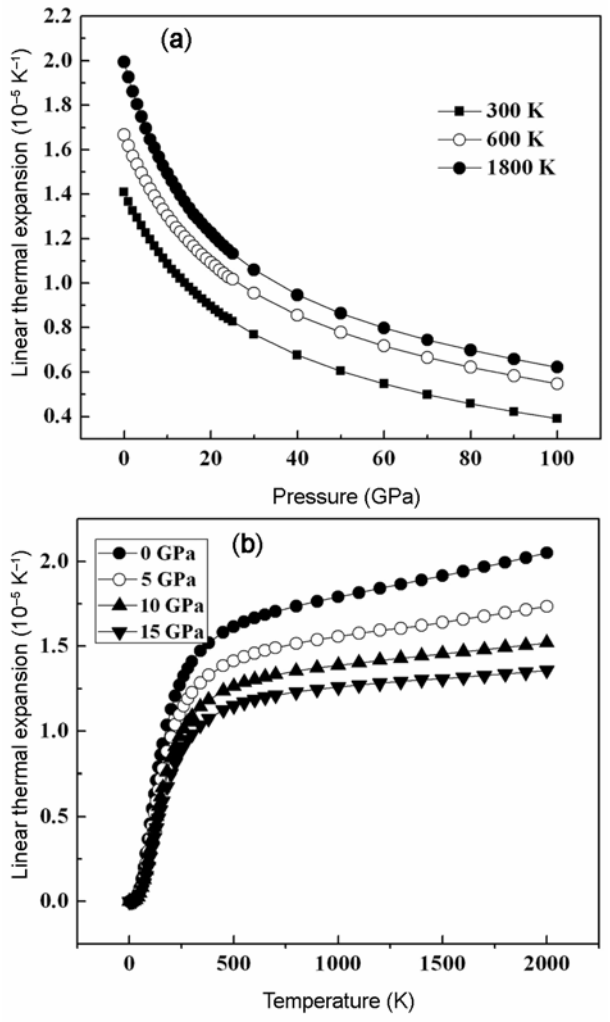

Figure 9. Variation of the thermal expansion coefficient α with (**a**) pressure P and (**b**) temperature T.

The dependence of the thermal expansion α with the temperature T and pressure P are shown in figure 9. Our calculated α are slightly bigger than the ones in Kulkarni *et al* (2009) and Scabarozi *et al* (2009) (table 1). The effects of the pressure P on the thermal expansion coefficient α are obvious (figure 9a). However, it is noted that as the pressure increases, α almost decreases exponentially. This means that there is a large thermal expansion at low pressure, which is in accordance with the variation of V/V_0 with pressure P. In figure 9b, it can be seen that the thermal expansion coefficient α also increases with T^3 at lower temperatures and gradually approaches to a linear increase at higher temperatures, which is similar to that of C_V.

In figure 10, the heat capacity of Ti_2SC is plotted for various pressures at different pressure i.e. 0, 30, 60, 90 and 120 GPa, respectively. It shows that when $T < 500$ K, the heat capacity C_V is sensitive to both the pressure P and the temperature T. This is due to the anharmonic approximations of the Debye model. However, at higher

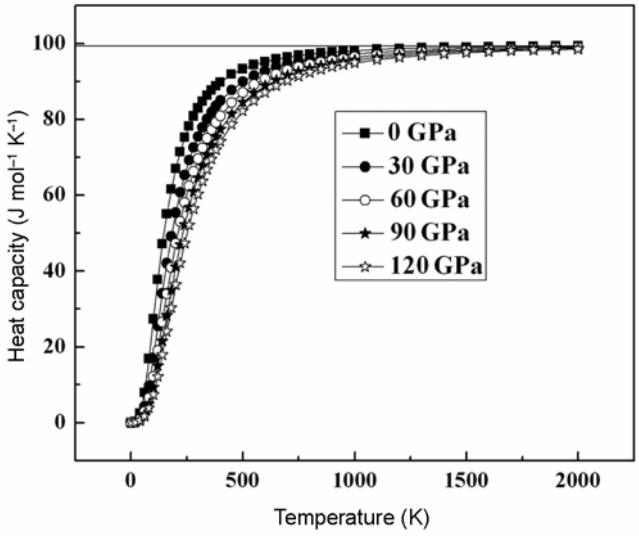

Figure 10. The heat capacity of Ti_2SC at various pressures and temperatures.

pressures and/or higher temperatures, the anharmonic effect on C_V is suppressed, and C_V is very close to the Dulong–Petit limit.

4. Conclusions

We have focused our attention on the elastic constants and anisotropy as well as thermodynamic properties under high pressures by using plane wave pseudopotential density functional theory within the generalized gradient approximation. We have obtained the pressure dependence of structural parameters V/V_0 performing total energy calculations over a range of the primitive cell volumes. The results are in agreement with experimental data. The pressure dependences of elastic constants and heat capacity are also obtained. It is found that the elastic constants, anisotropy and Debye temperature increase with pressure. It is found that its axial compressibility β and thermal expansion coefficient α decrease when increasing pressure; while the anisotropy factor, the c-axis and in-plane bulk moduli, and Debye temperature increase with pressure. The anisotropy can be explained by the strong Ti–S hybridization and weak C–C hybridization.

Acknowledgements

This project was supported by the National Natural Science Foundation of China under grant No. 40804034, and by the Natural Science Foundation of the Education Department of Henan province of China under grant nos 2009B590001 and 2007140011, by Henan Science and Technology Agency of China under grant no. 092102210314 and by Open Project State Key Laboratory of Superhard Materials (Jilin University) No. 201107.

References

Amini S, Barsoum M W and Raghy T E 2007 *J. Am. Ceram. Soc.* **90** 3953

Anderson O L 1963 *J. Phys. Chem. Solids* **24** 909

Auld M A 1973 *Acoustic fields and waves in solids* (New York: Wiley) **Vol 1**

Barsoum M W 2000 *Prog. Solid State Chem.* **28** 201

Barsoum M W and Raghy T E 1996 *J. Am. Ceram. Soc.* **79** 1953

Barsoum M W and Raghy T E 1997 *J. Mater. Synth. Process.* **5** 197

Barsoum M W and Raghy T E 1999 *Metall. Mater. Trans.* **A30** 1727

Blanco M A, Francisco E and Luaña V 2004 *Comput. Phys. Commun.* **158** 57

Born M 1940 *Proc. Cambridge Philos. Soc.* **36** 160

Bouhemadou A and Khenata R 2008 *Phys. Lett.* **A372** 6448

Cui S X, Feng W X, Hu H Q, Feng Z B and Liu H 2009 *Scripta Mater.* **61** 576

Drulis M K, Drulis H, Hackemer A E, Ganguly A, Raghy T E and Barsoum M W 2007 *J. Alloys Comput.* **433** 59

Du Y L, Sun Z M, Hashimoto H and Tian W B 2008 *Phys. Lett.* **A372** 5220

Francisco E, Recio J M, Blanco M A, Martín Pendás A and Costales A 1998 *J. Phys. Chem.* **A102** 1595

Fu H Z, Hua L D, Feng P, Gao T and Lu C X 2008a *Commun. Theor. Phys.* **50** 1427

Fu H Z, Hua L D, Feng, P, Gao T and Lu C X 2008b *Comput. Mater. Sci.* **44** 774

Fu H Z, Liu W F, Peng F and Gao T 2009 *Physica* **B404** 41

Hug G 2006 *Phys. Rev.* **B74** 184113

Islam A K M A, Sikder A S and Islam F N 2006 *Phys. Lett.* **A350** 288

Karki B B and Ackland G J and Crain J 1997 *J. Phys. Condens. Matter* **9** 8579

Kulkarni S R, Merlini M, Phatak N, Saxena S K, Artioli G, Amini S and Barsoum M W 2009 *J. Alloys Compd.* **469** 395

Kulkarni S R, Vennila R S, Phatak N A, Saxena S K, Zha C S, Raghy T E, Barsoum M W, Luo W and Ahuja R 2008 *J. Alloys Compd.* **448** L1

Lippens P E, Chadwick A V, Weibel A, Bouchet R and Knauth P 2008 *J. Phys. Chem.* **C112** 43

Ma Y M, Eremets M, Oganov A R, Xie Y, Trojan I, Medvedev S, Lyakhov A O, Valle M and Prakapenka V 2009 *Nature* **458** 182

Manoun B, Gulve R P, Saxena S K, Gupta S, Barsoum M W and Zha C S 2006 *Phys. Rev.* **B73** 1

Milman V, Winkler B, White J A, Packard C J, Payne M C, Akhmatskaya E V and Nobes R H 2000 *Int. J. Quantum Chem.* **77** 895

Murnaghan F D 1994 *Proc. Natl Acad. Sci. USA* **30** 244

Neumann G S, Stixtude L and Cohen R E 1999 *Phys. Rev.* **B60** 791

Nye J F 1985 *Physical properties of crystals: their representation by tensors and matrices* (Oxford: Clarendon)

Perdew J P, Burke K and Ernzerhof M 1996 *Phys. Rev. Lett.* **77** 3865

Poirier J P 2000 *Introduction to the physics of the earth's interior* (Cambridge: Cambridge University Press)

Scabarozi T H, Amini S, Finke P L, Leaffer O D, Spanier J E, Barsoum M W, Tambussi W M, Hettinger J D, Drulis M and Druli H 2008 *J. Appl. Phys.* **104** 033502

Scabarozi T H, Amini S, Leaffer O, Ganguly A, Gupta S, Tambussi W, Clipper S, Spanier J E, Barsoum M W, Hettinger J D and Lofland S E 2009 *J. Appl. Phys.* **105** 013543

Segall M D, Lindan P L D, Probert M J, Pickard C J, Hasnip P J, Clark S J and Payne M C 2002 *J. Phys. Condens. Matter* **14** 2717

Sirdeshmukh D B, Sirdeshmukh L and Subhadra K G 2001 *A handbook of physical properties* (New York: Springer-Verlag)

Spanier J E, Gupta S, Amer M and Barsoum M W 2005 *Phys. Rev.* **B71** 012103

Steinle-Neumann G, Stixtude L and Cohen R E 1999 *Phys. Rev.* **B60** 791

Tetsuya S, Koich I, Toshiharu N, Katsunari O, Kiyohito I and Denki S 2002 *Electric Furnace Steel* **73** 379

Wallace D C 1972 *Thermodynamics of crystals* (New York: Wiley)

Wally P and Ueki M 1998 *J. Solid State Chem.* **138** 250

Yang H, Manoun B, Downs R T, Ganguly A and Barsoum M W 2006 *J. Phys. Chem. Solids* **67** 2512